A Generalized Methodology For Partial Volume Correction In Emission Tomography

Y. Ma, O. Rousset and A.C. Evans [1]
Montreal Neurological Institute and McGill University

Abstract

We describe a generic methodology to correct 3-D partial volume effects in clinical emission scans. It is based on prior knowledge of tracer biodistribution and tomographic imaging characteristics. We derive this information from registered and segmented MR/CT data. Two fast numerical algorithms are then used to estimate structure-specific recovery coefficients and activity spillover contributions. In this work we evaluate our method using MR/PET data acquired from a 3-D brain phantom. It is made of a human skull and plastic chambers to emulate radiotracer uptake in neuroreceptor imaging studies. Regional activity values among striatal structures are typically underestimated by 20-45 % depending on their spatial location. After correction they are restored to within 5 % of the true concentration. We also add several automatic steps to increase computational efficiency and simplify its usage in clinical environment.

I. Introduction

Partial volume effects originate primarily from the limited 3-D image resolution in PET/SPECT systems. This is a big problem because of irregular and dynamic activity distribution in the body. It will produce spatially variant imaging distortions and non-stationary bias and variance in time activity curves.

There exist many interests in image restoration methods to solve partial volume problems. In recent years it has been a common practice to analyze tomographic data using regional templates created from multimodality images [1]. This gives valuable information with proper image segmentation. We have seen increased use of correlated MR data in Bayesian image reconstruction [2, 3, 4]. This is the most fundamental approach which reconstructs each frame iteratively. It is not in routine clinical use due to high computational cost.

[1] A summary submitted to 1998 IEEE Medical Imaging Conference.

It is more desirable to employ non-iterative methods for the in-vivo correction of the 3-D partial volume effects in regional functional data. Some early algorithms rely on simple calculations in image space [5, 6]. However they require explicit estimates of background activity. While possible in some cases this is not always applicable in general clinical studies. We have developed an elegant method free from any unrealistic assumptions [7]. It works by estimating the magnitude of pure recovery and activity spillover between different functional entities in a given set of ROIs. In this paper we describe many improvements implemented to automate our method and make it independent of a particular tomograph.

II. Computational Method

It is known that the observed activity within a particular tissue is the weighted sum of the true activity from all the active tissues in the biological system. Assume there are N different tissues participating in the imaging experiment each with a relative homogeneous tracer uptake. Let vectors t_i and v_j denote the mean and variance measured from any sets of ROI templates. One can easily derive this relationship:

$$t_i = \sum_{j=1}^{N} \omega_{ij} T_j \qquad (1)$$

where ω_{ij} is the transfer matrix and T_j the true activity of each tissue. Note that the weighting factors ω_{ij} depend on activity distribution but independent of its concentration. This then represents a set of linear equations which can be solved to obtain the true regional values:

$$T_i = \sum_{j=1}^{N} \omega'_{ij} t_j \qquad V_i = \sum_{j=1}^{N} {\omega'_{ij}}^2 v_j \qquad (2)$$

where ω'_{ij} is the inverse matrix of ω_{ij} and V_i the variance of the corrected data. Both of them depend on 3-D image resolution and data analysis strategy.

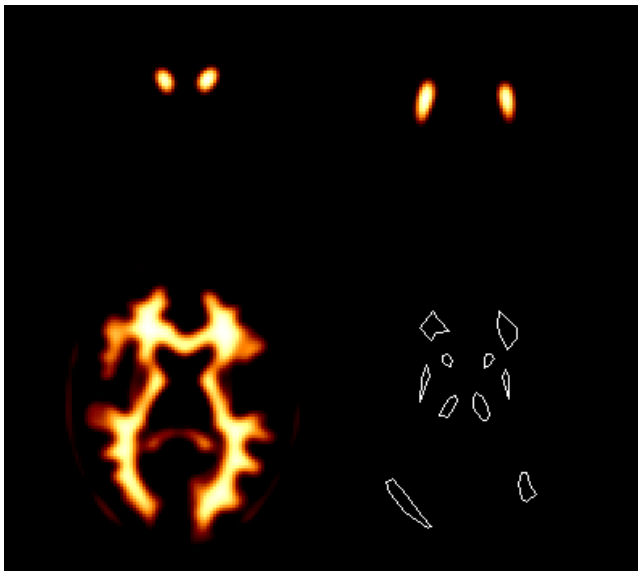

Fig. 1 Extraction of the transfer matrix from individual tissue maps and anatomical templates of the brain phantom.

Collectively ω_{ij} reflects the interaction of each tissue with the scanner and spillover effects among themselves. One can determine its elements only by accurate simulation of radiotracer distribution and 3-D tomograph resolution. We have already described a procedure to calculate them from 3-D anatomical maps [7]. Simulated images of each structure are generated separately and analyzed with the same ROI sets as in clinical scans. Fig. 1 shows a pictorial representation of this process. We then estimate the fraction of activity from the structure itself and that from its neighboring structures. Afterwards one can compute the true activity and variance values of each tissue by (2). We use the same matrix over all TACs extracted from dynamic images.

In our previous work we calculate the transfer matrix by going through the projection/backprojection of a multi-slice PET scanner. It can handle only a small number of structures with uniform tracer distribution. We have since incorporated many additional steps to make our programs faster and easy to implement. Now they work with any number of tissues with non-uniform tracer uptake. In particular we have implemented a 3-D convolution algorithm in image space. This allows us to compute the correction matrix based on 3-D image resolution of any tomographic systems but independent of their acquisition geometry. We can perform 3-D correction in dynamic TACs automatically with given anatomical maps and ROI sets.

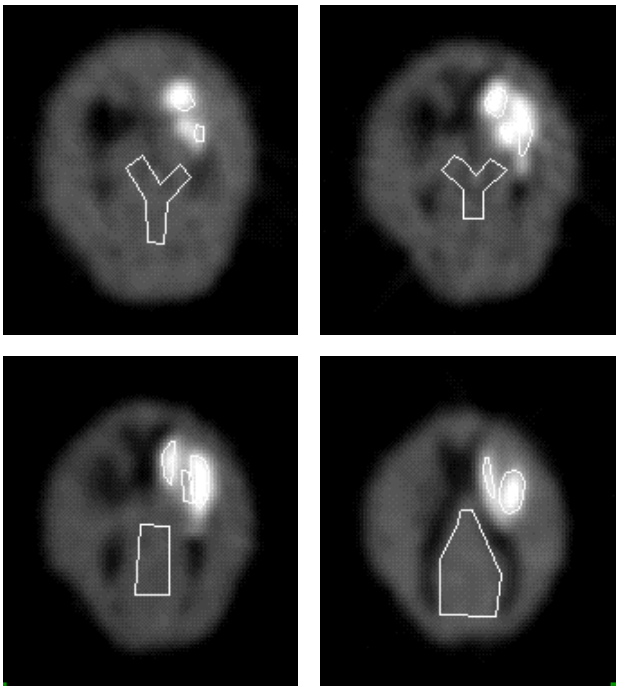

Fig. 2 Anatomical templates of the striatal structures and PET images of the skull phantom with a 6 mm Hanning filter.

III. Experimental Results

We evaluated the accuracy and precision of our algorithms by scanning a 3-D human skull phantom on MR and PET scanners. It contains separate compartments of striatum and ventricles enclosed in a main chamber. A uniform F-18 solution was filled in the regions of caudate nuclei (CN), putamen (PU) and globus pallidus (GP) with a warm background in the main cavity (BKG). After registration MR images were segmented into individual volumetric structures. We also drew irregular boundaries slightly inside each of them covering four PET slices in Fig. 2. With a 6.5 mm separation they have around 5 M counts. Areas of small ROIs vary from 52 - 288 mm^2 with large ones between 602 - 1566 cm^2.

We then extracted the mean activity and standard deviation within each structure which were further corrected according to (2). Both were converted into recovery coefficients using the true activity in each compartment. Table 1 shows sample results of one image in the middle of the phantom. As expected we observe most errors in the striatal structures. Our method improves the accuracy of activity estimates by more than 30% while increasing the coefficient of variation by about 50%. We see even larger biases in the measured data from other slices with substantial

Table 1
A typical transfer matrix of the skull phantom. Mean and variance data of the regional recovery coefficients before/after restoration.

ID	CN	PU	GP	BKG
cn	0.672	0.018	0.008	0.233
pu	0.037	0.483	0.112	0.358
gp	0.022	0.070	0.611	0.258
bkg	0.000	0.000	0.000	0.989
obs	0.726	0.693	0.756	0.971
std	0.060	0.095	0.023	0.124
corr	0.954	0.942	0.986	0.982
std	0.090	0.203	0.046	0.125

spatial variability. This comes from differences in the object size relative to the 3-D image resolution. Such errors are reduced to within about 5% after correction with tolerable noise amplification. Using procedures described in [8] we have done extensive simulations of dynamic PET studies with the human brain MRI data. Partial volume corrections show complete restoration of both the shapes of TACs and the extracted physiological constants.

IV. Conclusions

We have established a general methodology which is capable of removing 3-D partial volume distortions in dynamic emission studies using the correlated MR/CT images. The key element of this method is the estimation of tissue recovery and cross-contamination fractions by imaging each structure separately. After obtaining the promising results from dynamic PET data in the brain, we expect great improvement in imaging accuracy from cardiac scans as well. Its applications rely on the correct identification of the binding structures involved in the study and all the surrounding tissues with different kinetic properties. With our extensions it becomes usable in any user-selected imaging protocols and tomograph systems. This will reduce/eliminate regional quantitation errors due to scan-specific characteristics and anatomical differences.

V. References

[1] G.J. Klein, X. Teng, and W.J. Jagust et al. A methodology for specifying PET VOI's using multimodality techniques. *IEEE Trans. Med. Imag.*, 16:405–415, 1997.

[2] E.U. Mumcuoglu, R. Leahy, and S.R. Cherry. Bayesian reconstruction of PET images: methodology and performance analysis. *Phys. Med. Biol.*, 41:1777–807, 1996.

[3] J.E. Bowsher, V.E. Johnson, and T.G. Turkington. Bayesian reconstruction and use of anatomical a priori information for emission tomograph. *IEEE Trans. Med. Img.*, 15:673–686, 1996.

[4] S. Sastry and R.E. Carson. Multimodality Bayesian algorithm for image reconstruction in PET: a tissue composition model. *IEEE Trans. Med. Imag.*, 16:750–761, 1997.

[5] J.M. Links, J.K. Zubieta, C.C. Meltzer, M.J. Stumpf, and J.J. Frost. Influence of spatially heterogeneous background activity on hot object quantitation in brain ECT. *J. Comput. Assist. Tomogr.*, 20:680–687, 1996.

[6] H.R. Tang, J.R. Brown, and B.H. Hasegawa. Use of CT-defined regions for the determination of SPECT recovery coefficients. *IEEE Trans. Nucl. Sci.*, 44:1594–1599, 1997.

[7] O. Rousset, Y. Ma, and A.C. Evans. Correction for partial volume effects in PET: principle and validation. *J. Nucl. Med.*, 39:in press, 1998.

[8] Y. Ma and A.C. Evans. Analytical modeling of PET imaging with correlated functional and structural images. *IEEE Trans. Nucl. Sci.*, 44:2439–2444, 1997.